ISIJ International, Vol. 56 (2016), No. 7, pp. 1171–1180

Fundamental Forces Driving Analogue Sinter Mix Reshaping

Lauren ANDREWS,* Chin Eng LOO and Geoffrey EVANS

Centre for Ironmaking Materials Research, Discipline of Chemical Engineering, School of Engineering, Faculty of Engineering & Built Environment, The University of Newcastle, Callaghan, NSW 2308 Australia.

(*Received on February 4, 2016; accepted on March 17, 2016*)

Major structural change occurs during sintering on melt formation. Melts activate surface forces that drive coalescence processes, as surface energy is reduced. The extent to which coalescence occurs depends on the relationship between surface and viscous forces, which in turn are determined by composition and temperature. In this study, a coal ash fusion furnace was utilised to investigate the impact of composition and temperature on analogue sinter mix tablet reshaping over alumina tiles. Sinter mix compositions were comparable to small size fractions of plant sinter mixes; as they are the first to form melt during sintering operations. A factorial experiment showed basicity to be the dominant driver for reshaping with increasing temperature. Alumina was found to retard reshaping, but only at low sintering temperatures. Material properties, calculated using FactSage and published correlations, were determined as a way to investigate forces acting in the system. Results showed the main determinant of reshaping was apparent viscosity, which was primarily dependent on the amount of melt formed in the sinter mix. The study also used a novel experimental technique, which demonstrated the ability of surface forces to drive reshaping and surface energy reduction when the tablet was suspended from a downward facing tile. This study found that while melt surface tension and wetting behaviour drive system reshaping to reduce surface energy, the extent of sinter mix reshaping was predominately determined by resistance from viscous forces.

KEY WORDS: iron ore sintering; melt properties; viscosity; surface tension; FactSage.

1. Introduction

Iron ore sintering is an agglomeration process which converts fine iron ores (typically less than 9 mm) into a lumpy feed for the ironmaking blast furnace. The sinter mix, comprised of iron ores, fluxes and coke breeze, is granulated before being charged onto the moving sinter strand. In a granulating drum water is sprayed onto the sinter mix causing fine particles to layer onto the surfaces of coarser particles, forming granules (**Fig. 1**). As the bed travels under an ignition hood, coke particles on the top surface are ignited to form a narrow flame front. Suction applied at the bottom of the bed draws air through, causing the flame front to move downwards. In the flame front partial melting of the sinter mix occurs and the bed undergoes significant structural change, as agglomerated regions and large voids form. When the bed is fully sintered it falls onto a spike roll crusher, which releases these agglomerated (or sinter) particles.

Figure 1 illustrates structural differences between a green granulated bed and sintered bed. Coarsening the sinter mix through granulation improves the permeability of the green bed and distributes both larger (core) particles and inter-particle voids throughout the bed in a fairly uniform

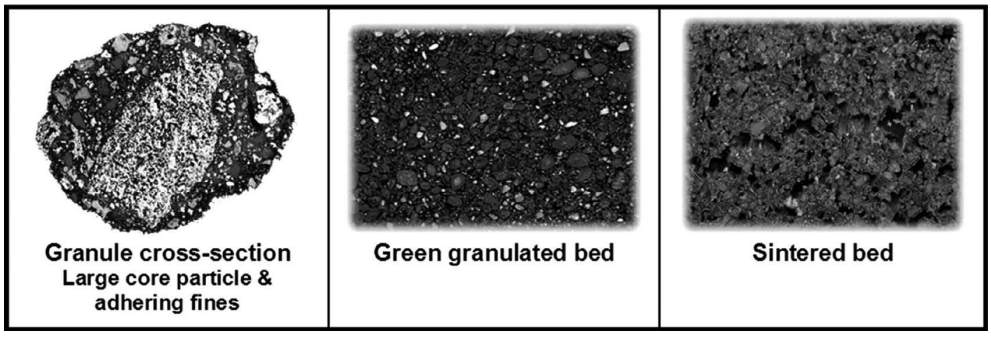

Fig. 1. Structural change within the sinter bed.

* Corresponding author: E-mail: lauren.andrews@uon.edu.au
DOI: http://dx.doi.org/10.2355/isijinternational.ISIJINT-2016-069

arrangement.[1] This is in contrast to the sintered bed that contains irregularly shaped and sized agglomerated regions amongst larger void networks. In the flame front temperatures as high as 1 350°C are reached and ferruginous melts form amongst ore particles. These melts promote coalescence, which is defined as "the physical process in the flame front that causes material to come together and form larger units"[2] (agglomerated regions). The extent to which the partially-molten mix coalesces within the flame front determines sinter properties such as size and strength, and these parameters subsequently influence the operation, stability and efficiency of the blast furnace.[1]

Coalescence occurs spontaneously on melt formation[3] as the three phase system (solid-melt-gas) moves to reduce surface energy at the micro and macro level. As agglomerated regions form in the flame front, the extent to which they continue to coalesce depends on the ability of melts to move these regions and their intra-pores towards sphericity, as well as driving pore coalescence and removal resulting in densification.[1] The main driver is the surface tension and wetting nature of melts,[4] with movement resisted by viscous forces.[5] Melt surface and viscous forces depend on many factors, and during sintering their magnitude changes throughout the bed due to local variations in temperature and composition.

Coalescence is complex and cannot be studied directly through tracking and quantifying material movement during sintering operations. Further, coalescence in iron ore sintering is not well understood and cannot be quantified using a specific measure or equation. Several approaches[1,5–7] have been adopted to investigate coalescence phenomenon. Sinter properties including size, density and pore properties have been used to understand and compare the degree of coalescence in laboratory-scale sinter tests.[1,5] However, these approaches have been unable to incorporate or quantify the impact of melt properties, which underlie coalescence behaviour.

This study aims to provide insight into how melt behaviour is impacted by composition, temperature and material properties, as a way to elucidate the mechanism of melt flow. Firstly, studies on coalescence have been reviewed, as well as the mechanism of melt formation within sintering operations; from which a suitable sinter mix composition was identified for experimental investigation into wetting and reshaping over a controlled (alumina) surface. Secondly, an experimental program has been undertaken in a Coal Ash Fusion (CAF) furnace, allowing the impact of composition and temperature on macro movement and reshaping of pressed analogue sinter mix tablets (on alumina tiles) at sintering temperatures to be assessed. The ability of sinter mix tablets to flow and reshape, due to melt formation, was a way to assess their ability to drive surface energy reduction and hence influence coalescence. The effect of changing the force balance was also explored using a novel experimental approach (see **Fig. 2**), where the tablet was suspended from a downward facing tile. Finally, the forces acting within the sinter mix tablets on heating were related to the observed reshaping of the tablet as well as material properties inferred from published correlations. A critical review of these correlations is also presented.

2. Literature Review

2.1. Coalescence

The amount and properties of the melts formed are the result of sintering reactions in the flame front, which are sensitive to local conditions within the sinter bed. With the passing of the flame front, melts solidify to form the bonding phase in the product sinter. Dawson *et al.*[8] (1984) showed how sinter bed temperature profiles vary with bed depth. As the flame front descends, both maximum temperatures and the width of the flame front (time at sintering temperatures) increase. They investigated the effect of heating fluxed iron ore tablets to different maximum temperatures and found significant changes in the resulting mineralogy, porosity and texture.

The first mention of the coalescence phenomenon within iron ore sintering was by Kasai *et al.*[6] (1989). Their investigation into coalescence involved theoretical analysis of the forces acting within the sinter bed and experimentally investigating coalescing behaviour of manufactured granules. They identified three important forces driving sinter bed structural change: compressive, frictional and capillary. These forces are the result of material mass in the packed bed, the flowing gas stream and the formation of a wetting liquid. The main forces driving structural change were found to occur from a balance between compressive and capillary forces. Experimental work utilised granules of nuclear particles surrounded by mixtures of fine iron ore and limestone (adhering fines). Groups of granules were heated to various sintering temperatures and the extent of coalescence determined from qualitative observation, based

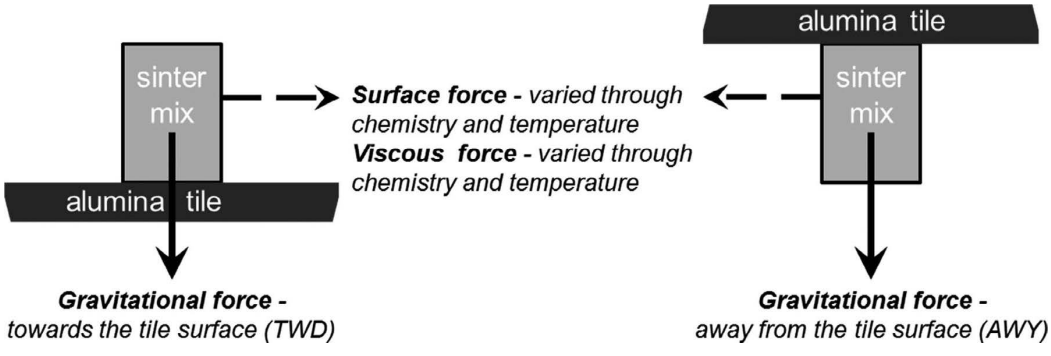

Fig. 2. Forces involved in sinter mix reshaping to reduce surface energy.

on the extent of granule fusion. The extent of coalescence was related to the viscosity of the adhering fines mixtures, which included the apparent viscosity of solid-melt mixtures when experimental temperatures were below liquidus temperatures. They also identified surface tension, melt viscosity and/or the apparent viscosity (melt-solid mixtures) to be essential factors to understand the coalescence mechanism. Calculations involving capillary forces and the viscosity of melts formed from the adhering fines layer were based on the binary calcium-ferrite system, which is a simplification of multicomponent sinter mixes.

Loo *et al.*[3] (1992) outlined the mechanism of melt formation within sintering. The general understanding is that the first or primary melts form within the adhering fines layer of granules; where the smallest particles are in close contact (see granule structure, Fig. 1). Secondary melts form as the nuclear particle is assimilated by the primary melt. The heterogeneous nature of the sinter bed results in local variations in both melt chemistry and temperature that affect material properties and hence coalescence. In spite of the local variations, they were able to demonstrate that primary melt formation can be investigated through using compositions comparable to the −0.5 mm fraction of plant sinter mixes.

Loo and Leung[5] (2003) heated a range of analogue sinter mixes under sinter temperature profiles to investigate the impact of composition and temperature on bonding phase micro-structure. Composition and temperature were shown to impact melt properties through their impact on bubble reshaping and coalescence, which were observed from the pore properties of the micro-structure. Temperature had a significant effect on the resulting porosity, with increasing temperatures showing increasing pore coalescence and rounding. However, due to limited data for sinter mixes results could not be quantified in terms of melt properties.

Yap *et al.*[7] (2007) utilised 2D image analysis techniques to investigate pore coalescence of analogue sinters. They found pore morphology (solidity) and area were the most suitable parameters for investigating micro coalescence, which also reflect melt properties.

Loo and Heikkinen[1] (2012) assessed sinter properties at different locations within a sinter bed and found that increasing sinter temperatures resulted in the production of denser sinter particles. The formation of more melt in the lower bed improved the ability of the system to coalesce.

Based on work by Kasai *et al.*,[6] the implication for structural change in the sinter bed is that the top of the bed primarily results from the capillary forces of sinter melts, while lower in the bed both capillary and compressive forces apply. Another consideration is that while the impact of the compressive force increases with increasing bed depth is also influenced by bed temperatures. Dawson *et al.*[8] showed temperatures increase down the bed and temperature impacts sinter density[1] and bonding phase micro-structure.[5]

2.2. Melt Properties

The present study investigates multicomponent sinter mixes that approximate primary melt formation (see Section 3) and analyses reshaping behaviour in relation to melt properties. Ferruginous melts generated during sintering differ to oxide melts in other metallurgical systems due to their high Fe_2O_3 content. Consequently, there is limited published data on material properties of melts encountered in iron ore sintering systems. However, software packages and mathematical models are available for various slag systems; some with broad application and these were investigated to determine appropriate correlations with which to assess experimental results, and are discussed below.

2.2.1. Surface Tension

Capillary forces drive structural change in the flame front, providing strong surface densification forces[9] that work to pull material together. The strength of capillary forces depends on both melt surface tension and how it wets ore particles.

The surface tension of oxide systems can be determined using an additive approach.[10] However, surface tension is a surface property rather than a bulk property; where surface active components alter the surface tension as they move from the bulk to the interface.[11] Mills and Keene[12] outlined a model for determining the surface tension of Basic Oxygen Steelmaking (BOS) slags at 1 500°C, which takes into account surface active components. The model is also applicable to multi-component industrial slags and can be used at various temperatures by applying a temperature coefficient model, which is based on the melt composition.[11] The experimental mixes in the present study contained one surface active component, hematite. As such, the equation to determine the surface tension of experimental melts is given by:

$$\gamma_T = \sum x_i\gamma_i + (T - 1\,773)\sum x_i\left(d\gamma_i/dT\right) \quad \text{..... (1)}$$

Where

- γ_T is the surface tension of the melt at temperature T,
- x_i is the mole fraction of component i, in the melt,
- γ_i is the partial molar surface tension for melt components, see **Table 1**
- T is the melt temperature, K
- $d\gamma_i/dT_i$ is the partial molar surface tension temperature coefficient for melt components, see Table 1

2.2.2. Wetting

Wetting is the term used to describe the equilibrium configuration of a three phase (solid-liquid-gas) system due to the balance between surface forces.[13] Young's equation describes the horizontal balance of surface energies; where θ_{eq} is the contact angle the liquid makes with the system

Table 1. Partial molar surface tension and temperature coefficients for melt components.[11,12]

Oxide	Al_2O_3	CaO	FeO	MgO	SiO_2	Fe_2O_3
γ_i (mN m^{-1}) @ 1 500°C	655	625	645	635	260	$(-216.2/x+516.2)^{\ddagger}$
dγ_i/dT (mN m^{-1}K^{-1})	−0.177	−0.094	0.1	−0.13	0.031	−0.05

‡ For $x_{Fe2O3} > 0.125$; which is applicable to this study. See Ref. 12) for x_{Fe2O3} other than > 0.125.

at equilibrium and γ is the surface energy (or surface tension)[14,15] for the three interfaces, see **Fig. 3**.

$$\gamma_{SV} = \gamma_{SL} + \gamma_{LV}\cos\theta_{eq} \quad \text{..... (2)}$$

The contact angle a liquid makes with a solid surface at equilibrium characterises how the liquid wets the solid. When the contact angle is less than 90° the liquid is described as wetting. Literature indicates that melts formed in iron ore sintering operations are wetting.[16]

Investigation of sinter mix tablet behaviour in the present study was conducted using an alumina tile surface, where the surface energy of the solid-vapour surface was held constant. Variations in the reshaping and spreading nature between sinter mixes could be compared. However, the effect of surface tension and wetting alone are not sufficient to explain observed differences in reshaping behaviour; viscous resistance, that retards movement, also needs to be considered. This is discussed further below.

Wetting melts formed during sintering will flow, reshape and interact with solid surfaces to minimise surface energy. A consequence of wetting liquids is the phenomenon of capillary rise, which has implications for melt behaviour and capillary forces that occur during sintering.

In the flame front partial melting occurs, which results in configurations where melts form liquid bridges between ore particles. The wetting nature of sintering melts[4,16] means they interact with ore particles to create capillary forces that work to pull the ore particles together. These capillary forces are proportional to the surface tension of the liquid.[17]

Another consequence of wetting liquids is their ability to maintain contact with solid surfaces against the force of gravity. This behaviour is utilised in detachment techniques for determining liquid surface tension, such as the drop weight method.[18] In the current study a novel technique is used to investigate surface forces in analogue sinter mixes. By changing the way the gravitational force acts on the experimental system (see Fig. 2), the ability of surface forces to hold sinter mixes on alumina tiles and drive surface energy reduction can be compared. Using this technique, sinter mix tablets are not constrained by the size of the solid surface, which means they can demonstrate their capacity to drive surface energy reduction by moving and reshaping over the surface of the tile, if surface forces are greater than the gravitational force.

2.2.3. Viscosity

While surface forces work to drive surface energy reduction, their ability to cause movement and reshaping is retarded by viscous forces. If viscous forces are greater than surface forces movement will not occur.

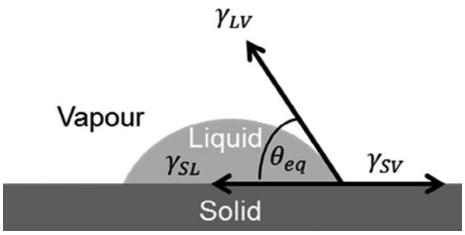

Fig. 3. Equilibrium contact angle and interfacial energy relationship (SV: solid-vapour, SL: solid-liquid, LV: liquid-vapour).

Local variations in composition and temperature throughout a sinter bed affect both melt surface tension and viscosity. However, when melts form during sintering they typically coexist with solid phases; which further increases their resistance to flow. The viscosity of a solid-melt mixture is termed 'apparent viscosity', and is a function of both melt viscosity and the volume fraction of solids within the melt. The present study investigates how melt viscosity and apparent viscosity affect sinter mix tablet behaviour.

There is limited experimental data published specifically on the viscosity of oxide melts found in iron ore sintering systems. The most comprehensive study to-date was by Machida *et al.*[19] who experimentally determined viscosities for slags similar to those found in iron ore sintering systems. However, application of their model to sintering systems is limited; requiring additional experimental data in order to verify model results.[19] There are however, mathematical models that determine viscosity based on structural parameters (due to the presence of different types of oxides) that apply to sintering melts, including FactSage[20] and CSIRO's MPE model.[21] The current study utilises the FactSage (Version 6.4) viscosity model.

Solid-liquid mixes that occur in sintering systems typically exhibit Bingham type flow;[9,22] where a yield strength must be overcome before flow can occur. For this type of flow the apparent viscosity can be determined using the Einstein-Roscoe equation for a two-phase (liquid-solid) system;[22]

$$\mu_A = \mu_0\left(1 - af\right)^{-n} \quad \text{..... (3)}$$

Where:

- μ_A is the apparent viscosity of the solid-melt mix,
- μ_0 is the viscosity of the melt,
- f is the volume fraction of solid particles in the melt,
- while a and n are constants.

Ideally the constants a and n would be fitted to experimental data. In the absence of experimental data however, suggested values of 1.35 and 2.5 respectively were used, which are for systems containing spherical particles. Application of the Einstein-Roscoe equation to the experimental sinter mixes requires knowledge of melt volumes.

Generally the molar volume of oxide systems can be determined using an additive approach, based on the mole fraction of components. However, certain oxides influence the molar volume based on their composition in the melt, including silica and alumina. Mills and Keene[12] outlined a mathematical model, developed for BOS slags, that takes into account these effects. The application of this model to iron ore sintering melts is reasonable as the model has broad application.[11,13]

2.3. Discussion

The main forces involved in driving the reshaping behaviour of sinter mixes on alumina tiles are surface, viscous and gravity. Surface forces work to reduce surface energy in the system, while viscous forces oppose movement. When the gravitational force is towards the tile (TWD, see Fig. 2) it works with surface forces to drive reshaping. However, when the direction of the gravitational force is away from the tile (AWY, see Fig. 2) the ability to maintain contact with the tile and reshape to reduce surface energy depend

on the strength of surface forces. Under such conditions it is expected that the reduction in tablet height will not be as large as when gravity works with reshaping. Further, if surface forces are not strong enough, tablet height could increase as the viscous resistance decreases and the tablet elongates. If surface forces are too low, the tablet will detach from the alumina tile.

Studies to date have not provided a methodology that directly quantifies the impact of pore coalescence within sinter mixes. After heating, the resulting sinter mix tablet volume is the sum of the solids volume (including solid phases and solidified melt) and gas volumes from remaining pores. The gas volume can be considered as the outcome of coalescence from when the melt was in liquid form, which also relates to densification within the sinter mix. Assuming tablets maintain contact when the gravitational force is away from the tile, differences in coalescence behaviour could be investigated through understanding how tablet volumes are impacted by changing the force balance.

3. Experimental

3.1. Design of Experiment

Loo and Leung[5] showed basicity, non-iron oxide content and alumina had a large impact on the resulting microstructure of sinter bonding phases in terms of pore size, shape and area. The present study assesses the impact of these three factors using a designed experiment approach; where factors vary independently of each other to prevent confounding and interaction effects can be assessed. Factors used in the present study include:

- gangue level (non-iron oxide content),
- alumina in the gangue (percent of non-iron oxide content), and
- basicity (wt% CaO/wt% SiO_2)

The reference chemical composition in this study is comparable to the composition of small size fractions of plant sinter mixes, which can be used to approximate primary melt formation[3] and is shown in **Table 2**. The experimental inference space is bounded by the settings chosen for the factors and is shown in **Table 3**. Sintering temperatures were investigated in 5°C intervals from 1 300°C up to a maximum of 1 350°C.

Table 2. Composition of midpoint chemistry.

	wt% Total	wt% in Gangue
Fe_2O_3	79.19	N/A
CaO	12.05	57.90
SiO_2	6.02	28.93
Al_2O_3	2.19	10.52
MgO	0.55	2.64

Table 3. Experimental inference space for factors investigated.

Factor	Low	Mid	High
Gangue level, wt% (non Fe_2O_3 content)	18.8	20.8	22.8
Alumina in gangue, wt%	8.5	10.5	12.5
Basicity (wt% CaO/wt% SiO_2)	1.5	2.0	2.5

3.2. Preparation of Sinter Mix Tablets

Analytical grade chemical powders used in the preparation of sinter mix tablets included: hematite (Fe_2O_3); limestone ($CaCO_3$); kaolinite ($Al_2Si_2O_5(OH)_4$); silica (SiO_2); and magnesium carbonate ($MgCO_3$). Chemicals were dried, weighed and homogenously mixed to the required compositions. Sinter mix tablets, each weighing approximately 0.4 g, were made using a cylindrical die with 6 mm internal diameter. A Shimadzu AGS-10kND press applied 200 N to each tablet.

To minimise experimental error two replicates of each compositon (for a total of three runs) were tested, which were made and tested in random order to avoid confounding results by systematic and/or equipment error.

3.3. Melt Flow on Alumina Tiles

Tablets were heated in a Carbolite Coal Ash Fusion (CAF) Digital furnace, with an internal work tube diameter of 79 mm and a maximum temperature of 1 600°C. A CCD camera fitted to the front of the furnace captured images of the tablets as they reshaped, as shown in **Fig. 4**. Images were recorded from 800°C at 1°C intervals.

Sinter mix tablets were placed on alumina tiles and positioned in the CAF furnace on a sample holder as shown in Fig. 4. A controlled alumina tile surface was used to isolate the impact of primary melt formation on sinter mix behaviour, without the complexity of assimilation reactions that occur with iron oxides during sintering. Tablets were heated at 6°C min^{-1} under an air atmosphere (supplied at 3 psi_g and 1 L min^{-1}) to 1 350°C and held for 1 minute to ensure 1 350°C was reached. Images of the tablets were assessed, with tablet height found to be the most reliable and reproducible response variable.

3.4. Melt Flow when the Tablet is Below the Tile

Two heating stages were required. The first was to adhere sinter mix tablets to the alumina tiles. While the second was

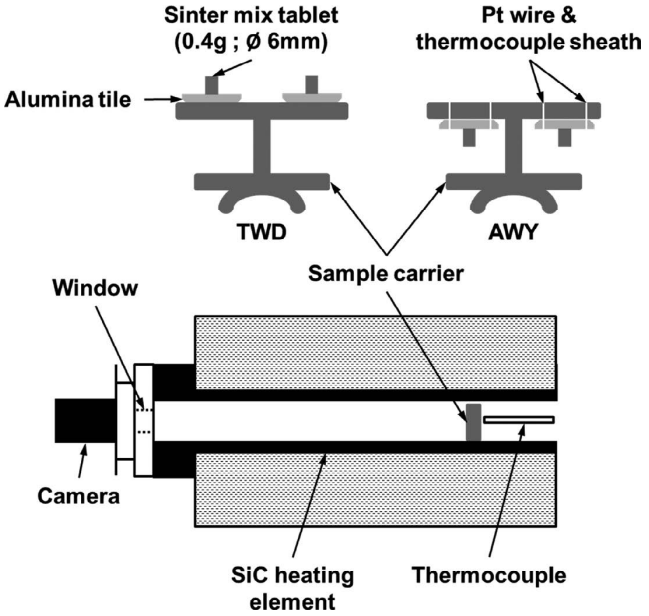

Fig. 4. Schematic diagram of experimental apparatus.

to assess flow and reshaping of sinter mix tablets, at sintering temperatures, when the gravitational pull was away from the tile (see Fig. 2).

Sinter mix tablets were heated under the conditions outlined in Section 3.3; except heating stopped at 1 290°C. At this temperature tablets adhered to the tile with limited flow and reshaping. However, samples with both high alumina and high basicity required 1 295°C to adhere to the tile. Once the tablets had cooled they were removed from the furnace.

Platinum wire and thermocouple sheaths were used to secure the alumina tiles so tablets faced downward as shown in Fig. 4. Thermocouple sheath was used to cover the platinum wire, reducing glare in the furnace images. Tablets were then heated under the same conditions outlined in Section 3.3.

3.5. Experimental Response

Furnace images were assessed using Zeiss axio-vision software to obtain pixel heights for each tablet. Tablet pixel height was normalised to allow comparison between tablets of different furnace runs. Tablet height was reported as a ratio of pixel heights, where the reference height was at 1 100°C (before melt formation).[23)]

3.5.1. Statistical Analysis of Experimental Response

An advantage of using a designed experiment approach is that results can be statistically assessed to determine the impact each experimental factor has on the experimental response. The impact of experimental factors (gangue level, basicity and alumina in the gangue) on tablet height was assessed using Minitab 15, where analysis was carried out at 5°C increments. The analysis provided correlations at each temperature interval. These correlations provided coefficients (ε^2) for each experimental factor, which represented the influence of the factor on the experimental response, and whether its effect on height reduction was positive or negative.

3.6. FactSage

Sinter mixes are multi-component and calculations to determine melt formation on heating are complex. When sinter mixes are heated, melts start forming amongst solid phases, and with increasing temperature the mass and compositions of solid and melt phases change. To investigate sinter mix melt formation FactSage[20)] (version 6.4), a thermochemical software and database package, was employed. FactSage features a Gibbs energy minimisation module that determines complex heterogeneous equilibrium for multi-component systems. The Gibbs module was used to determine equilibrium composition and mass data for liquid (melt) and solid phases for experimental sinter mix compositions, which were used to calculate material properties, at experimental temperatures.

4. Results and Discussion

4.1. Effect of Composition and Temperature on Tablet Height

Tablet height has been plotted as a function of temperature in **Fig. 5** for each of the nine experimental chemistries. Results for each composition are the average of three experimental runs, which showed good reproducibility. Compositions in the legend refer to whether the setting was high (H), low (L) or the midpoint (M) for gangue, alumina in the gangue, and basicity respectively. To assist with interpreting results in Fig. 5, the contribution of each experimental factor (ε^2) on tablet height as a function of temperature was also plotted and is displayed in **Fig. 6**. Results are discussed below in terms of basicity, gangue, alumina in the gangue, and temperature. It is noted that the statistical analysis did not identify any significant interactions between factors in the experimental inference space.

4.1.1. Basicity

Results in Fig. 5 show greater reduction in height at high basicity levels, followed by the mid basicity level, with low basicity compositions displaying the least reduction in tablet height. Results in Fig. 6 confirm that basicity is the dominant influence on tablet height for temperatures above 1 310°C. Information in the literature[3,5,24)] indicates basicity impacts sinter mix liquidus temperatures, with higher basicity resulting in lower liquidus temperatures. Although liquidus temperatures were not reached in the present study, basicity levels may impact the extent of partial melting, and hence the fluidity within sinter mixes, to drive tablet height

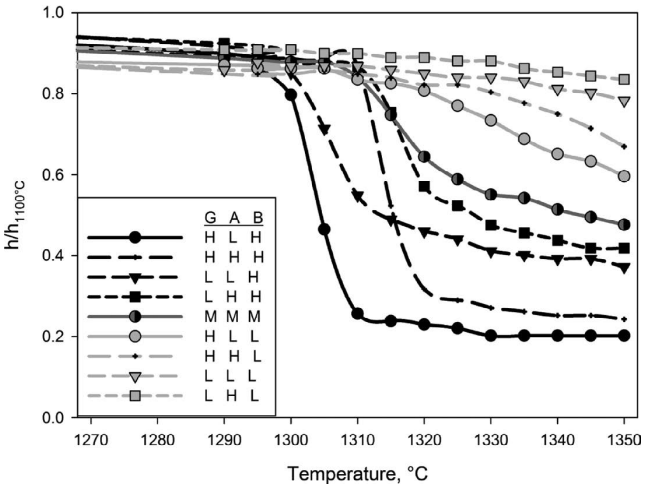

Fig. 5. Change in tablet height with temperature (G = gangue, A = alumina in gangue, B = basicity).

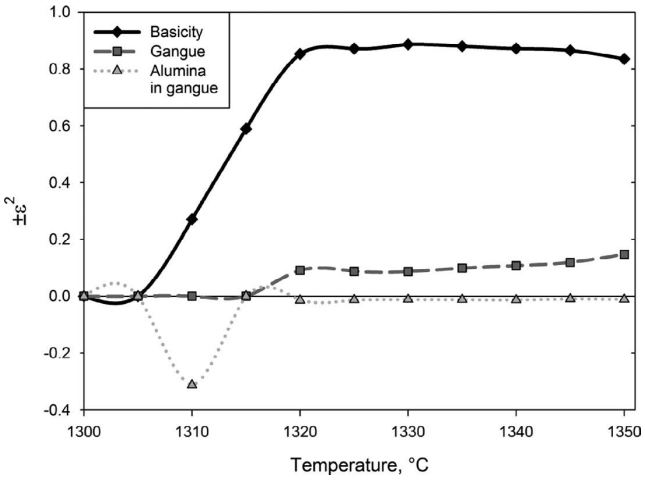

Fig. 6. Impact of experimental factors on tablet height.

reduction.

4.1.2. Gangue

Within a basicity group (high or low) the effect of gangue levels can be compared, see Fig. 5. In both the high and low basicity group, tablets that showed greater height reduction had high gangue levels. Results in Fig. 6 show that while basicity is the main determinant of tablet height reduction, gangue levels also contribute, at temperatures above 1 320°C. These results agree with information in the literature,[5] which indicates that increasing gangue levels also have the effect of reducing the liquidus temperature.

4.1.3. Alumina in the Gangue

When the only difference between a pair of compositions (in Fig. 5) is the amount of alumina in the gangue (*e.g.* HHH and HLH), the effect of alumina is apparent. In each case the sinter mix with high alumina in the gangue resulted in less reduction in tablet height. Results in Fig. 6 show that at lower sintering temperatures, between 1 305 and 1 315°C, alumina had a negative effect (retarding tablet height reduction), which was also observed in Fig. 5 (see HLH versus HHH).

Results in the literature[5] suggest small changes in alumina levels do not have a significant effect on the liquidus temperature. However, the effect on pore microstructure (at 1 300°C) was significant,[5] with increasing alumina levels increasing the overall pore area, which indicated a lack of fluidity. Results in Fig. 6 agree with the literature, as alumina was found to retard tablet height reduction at lower sintering temperatures (between 1 305 and 1 315°C), which is consistent with the effect on pore microstructure. While at higher temperatures alumina in the gangue did not have a significant impact on tablet height, which was consistent with the limited impact on liquidus temperature.

4.1.4. Temperature

Figure 5 shows that tablet height reduction increased as temperature increased, however temperature alone did not indicate the extent of reduction in tablet height as composition was a significant factor. At the maximum temperature of 1 350°C all compositions showed a reduction in height, however, the composition determined the extent. It is to be expected that increases in temperature would drive tablet height reduction, but its impact may be related to the proximity of the liquidus temperature, which depends on composition.

4.2. Effect of Sinter Mix Material Properties on Tablet Height

Composition and temperature were found to impact the reshaping ability of sinter mix tablets. While these effects were attributed to melt formation, they alone cannot define how melt formation impacts material properties and hence reshaping. Movement and reshaping could be due to changes in melt volume, melt viscosity, surface forces or combinations of these effects. As such, sinter mix material properties were determined to investigate how the forces acting within analogue sinter mix tablets impacted the reduction in tablet height.

4.2.1. Melt Mass

FactSage was used to predict the mass of melt formed in each of the nine sinter mix compositions at temperature. **Figure 7** shows how experimental results for each replicate over all nine compositions (between 1 320 to 1 350°C) correlate with the mass of melt. Analysis over this temperature range allows investigation of temperature effects, as the influence of other experimental factors have stabilised at 1 320°C, as shown in Fig. 6. A strong correlation exists, where 96% of the variation in the experimental response can be explained by the mass of melt formed within the tablet. As melt formation increases there is a greater reduction in tablet height. Results suggest that the amount of melt formed plays a significant role in driving movement and reshaping.

4.2.2. Melt Viscosity

Figure 7 also shows that over the experimental temperature range none of the compositions reached their liquidus temperature. FactSage was used to obtain mass and composition data of the melt and solid phases at experimental temperatures. The viscosity of the melt phase was calculated using the FactSage viscosity model. In terms of general trends, experimental results for height reduction were consistent with FactSage predictions for melt viscosity. However, the correlation was not as strong as for the mass of liquid, nor was the spread of viscosity values as large.

4.2.3. Apparent Viscosity

Apparent viscosity combines the effects of solids volume and melt viscosity and as such may provide a better indicator of tablet behaviour. The apparent viscosity of analogue sinter mixes was determined using the Einstein-Roscoe equation for a two-phase (melt-solid) system.[22] The volume fraction of melt and solid phases were determined through converting FactSage composition and mass data to volumes. Solid species were converted to volumes using density data, while a mathematical model, outlined in Section 2, was used to predict melt molar volumes.

Tablet height was plotted as a function of apparent viscosity and is displayed **Fig. 8** over the temperature range 1 320–1 350°C. Figure 8 demonstrates a logarithmic trend

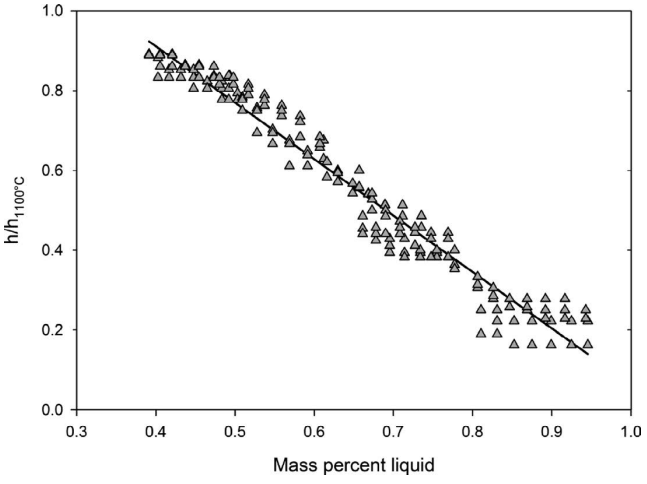

Fig. 7. Sinter mix tablet height versus mass of liquid (1 320–1 350°C).

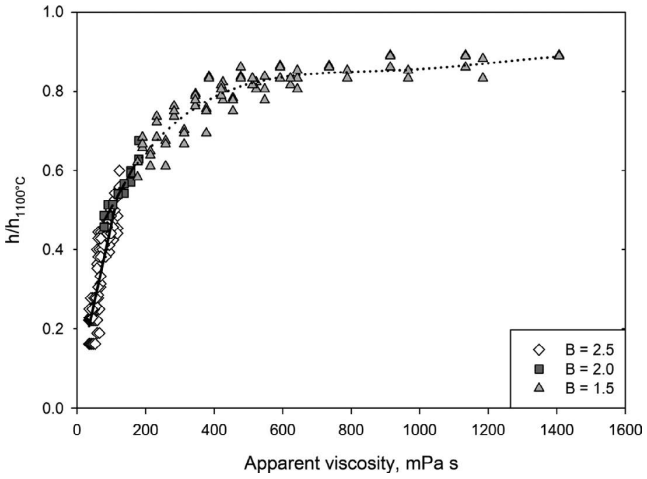

Fig. 8. Sinter mix tablet height versus sinter mix apparent viscosity (1 320–1 350°C).

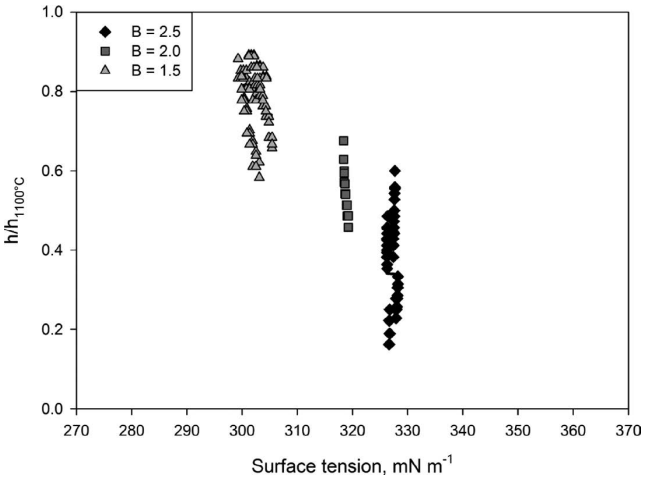

Fig. 9. Sinter mix tablet height versus melt surface tension (1 320–1 350°C).

in the relationship between tablet height and apparent viscosity; where small changes at low apparent viscosities correspond to large changes in tablet height, while large changes at high apparent viscosities result in small changes in tablet height. Low apparent viscosity values correspond to high basicity (2.5) compositions, while high apparent viscosities correspond to low basicity (1.5) compositions. The midpoint basicity (2.0) composition has apparent viscosity values that overlap between the two basicity levels. These findings are consistent with results that were analysed in terms of experimental factors (Section 4.1), which showed basicity to be the dominant influence for reduction in tablet height. Apparent viscosity is sensitive to the solids content (volume) and as such results in Fig. 8 suggest differences in tablet height reduction are predominately driven by basicity levels, which impact sinter mix melt volume.

4.2.4. Surface Tension

The surface tension of melts formed on heating the sinter mix tablets were calculated using Eq. (1), outlined in Section 2.2.1, using FactSage melt composition data. Sinter mix tablet height was plotted for each basicity level as a function of surface tension in **Fig. 9** over the temperature range 1 320–1 350°C. Within a basicity group there is little variation in surface tension compared to the change in tablet height (which corresponds to increasing temperatures as tablet height reduces). Even between basicity levels, the spread of results is not significant. The trends shown in Fig. 9 correspond to findings in literature for calcium ferrite melts that show little temperature dependence for a given composiston[25] and limited variation between chemistries at the same temperature.[25,26] Results suggest that while surface tension is important to driving surface energy reduction, it is not the dominant factor that determines the extent of reshaping.

Calculated surface tensions (0.3 N m^{-1}) were much lower than experimental values of 0.5–0.6 N m^{-1} reported in literature for melts similar to those found in sintering.[25,26] Melts in the present study had one surface active component, hematite. Since hematite is a major component of the melts, it had a large impact on surface tension values. While the surface tension correlation used in this study is applicable for multi-component industrial slags,[11] it may not be as accurate when dealing with sintering melts, which are significantly higher in hematite. However, calculated values may be used to investigate relative trends and differences between melt compositions.

4.2.5. Variation in Results

Knowledge of the physical properties of sinter mixes provides greater insight into factors driving material movement compared to composition and temperature alone. Surface tension is essential in driving surface energy reduction; however it showed little correlation to the experimental results. Much stronger correlation was observed for factors that relate to viscous forces including apparent viscosity and the mass of melt. These results suggest analogue sinter mix tablet movement is primarily determined by viscous forces rather than surface tension. In terms of sintering operations, viscous forces would also be expected to have significant impact on structural change.

A concern in tablet reshaping is the potential for segregation between solid and liquid phases due to melt formation and flow on the alumina tile. Segregation would cause localised variation in the composition of the sinter mix tablet and hence impact material properties as flow occurs; where the composition of melt that flows on the tile differs to the remaining sinter mix. In cases where segregation occurs, direct application of material properties determined using FactSage (thermodynamic) data would be limited. However, general trends can still be observed.

4.3. Effect of Changing the Vertical Orientation of the Tile Surface

Results of sinter mix tablet behaviour when the gravitational force is AWY from the tile are discussed below. Three experimental runs at each sinter mix composition were tested.

4.3.1. Impact of Composition on Reshaping Behaviour

As tablets were heated their viscous resistance decreased due to increased melt formation. Results in Section 4.2 showed there was a large difference in the viscous force between sinter mixes at sintering temperatures. By changing the gravitational force to act AWY from the tile, differences

in the viscous resistance became more apparent. **Figure 10** compares compositions that showed the greatest (left) and least (right) reduction in tablet height when the gravitational force was TWD the tile. Both sinter mix tablets maintained contact with the alumina tile on heating, demonstrating different reshaping behaviour. The tablet on the right did not appear to change shape, while the tablet on the left (HLH) showed significant reshaping. The fluidity of HLH appeared to increase above 1 305°C allowing the tablet to elongate as the viscous resistance decreased, increasing the ratio of surface to viscous forces. Subsequently, the surface force worked to pull the sinter mix towards the tile, reducing the surface energy of the system. This phenomenon occurred in the two chemistries that showed the greatest reduction in height (HHH and HLH), and is discussed below.

4.3.2. Comparing the Effect of the Gravitational Force on Tablet Height

Results for tablet height, both TWD and AWY from the tile, have been plotted as a function of temperature in **Fig. 11**, to investigate the effect of the gravitational force. Results show the average of three experimental runs for each case. In the runs where the gravitational force was AWY, both sinter mix tablets elongated as the viscous resistance was reduced due to melt formation. Elongation occurred at temperatures that corresponded with the largest change in tablet height when the gravitational force was TWD the tile. Consequently, the largest change in tablet height for the AWY runs required higher temperatures than the TWD runs. In each sinter mix case, final tablet heights for the AWY runs were higher than the TWD runs, which was attributed to the effect of the gravitational force working against or with surface energy reduction. Results in Fig. 11 show the ratio of surface to viscous forces is important to tablet reshaping.

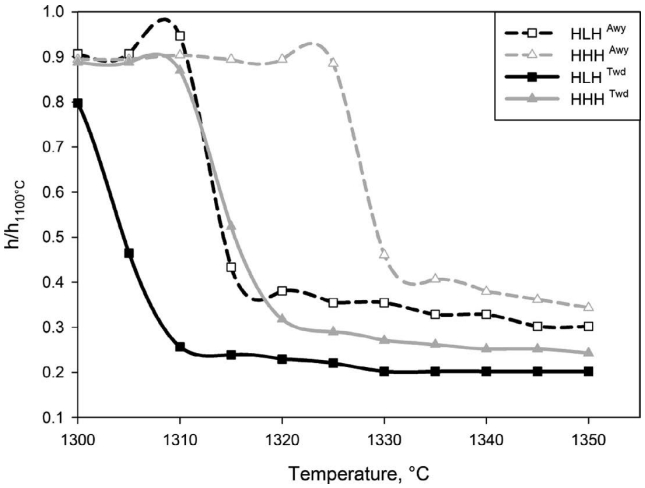

Fig. 11. Comparison between melt reshaping with and against gravity versus temperature.

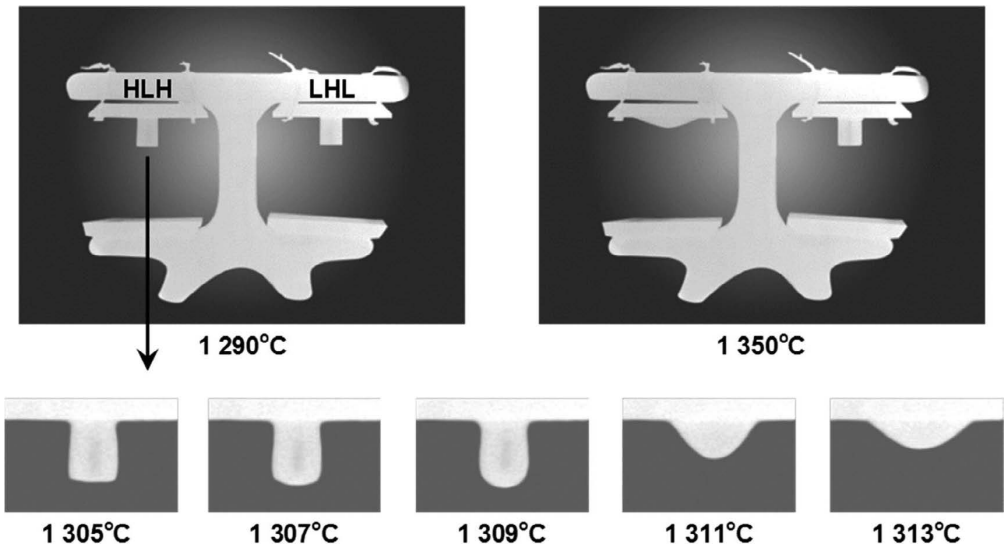

Fig. 10. Ability of sinter melts to maintain surface contact and reshape against gravity.

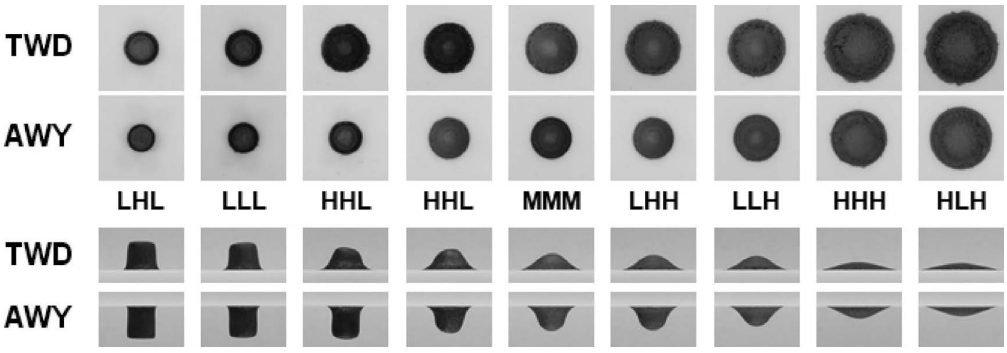

Fig. 12. Impact of the gravitational force on sinter mix reshaping after heating to 1 350°C.

4.3.3. Comparison of Tablet Reshaping and Spreading

A comparison of tablet reshaping (for all nine compositions) due to changing tablet orientation is shown in **Fig. 12**. In terms of height reduction, reshaping and spread over a tile, tablets showed consistent behaviour between sinter mixes. Though, as expected, for each composition there was less reshaping for tablets AWY. Results demonstrate the strength and significance of surface forces (that occur on melt formation) in maintaining contact with alumina tiles and driving surface energy reduction. However, they do not account for the large variation in reshaping between sinter mixes, as variation in melt surface tension was limited (Section 5.3). Sinter mix tablet flow AWY from alumina tiles also suggests viscous forces are the controlling force that determines the extent of sinter mix tablet reshaping.

5. Conclusions

Laboratory-scale experiments, in a Coal Ash Fusion furnace, were carried out to study the effects of melt formation on analogue sinter mix tablet reshaping. Sinter mix compositions tested were comparable to small size fractions of plant sinter mixes; which are the first to form melts during sintering operations. Tablet flow and reshaping are the result of surface, gravity and viscous forces that occur on melt formation, and reflect their ability to drive surface energy reduction.

A factorial experiment showed basicity to be the dominant driver for reshaping with increasing temperature. Alumina was found to retard reshaping, but only at low sintering temperatures. While composition and temperature were shown to have a large impact on tablet reshaping, they do not provide insight into the forces driving this behaviour.

A search of published correlations on material properties was conducted to determine correlations that could be applied to experimental compositions. FactSage was used to determine equilibrium compositions and mass of melt and solid phases at sintering temperatures, and as such provided the basis for estimating material properties. Results showed viscous forces were the main determinant of analogue sinter mix tablet movement, rather than surface forces. However, a novel experimental technique that changed the direction of the gravitational force, relative to sinter mix tablet reshaping, demonstrated the significance of surface forces. Surface forces worked to maintain tablet contact with alumina tiles, while also driving reshaping behaviour to reduce surface energy.

The novel experimental technique also demonstrated the impact of gravity on sinter mix tablet densification through the resulting tablet volumes after heating. Qualitative observation between sinter mixes of the same chemistry showed smaller tablet volumes resulted when the gravitational force was toward the tile surface. Differences in tablet volume are due to gas volumes, which are a function of the number and size distribution of pores. As such, the experimental technique could provide a method by which to assess bubble coalescence.

Sinter mix tablet reshaping was studied at sintering temperatures to understand the impact of melt properties. This study found that while melt surface tension and wetting behaviour drive surface energy reduction, the extent of sinter mix tablet reshaping was primarily determined by resistance from viscous forces.

Acknowledgements

Financial support from the Australian Research Council, BHP Billiton and Blue-Scope Steel is gratefully acknowledged. The authors would also like to thank Dr S. Chew for guidance with FactSage, Mr G. Penny for assistance with experimental work and preparation of graphs and Ms L. Matthews for preparing the images.

REFERENCES

1) C. E. Loo and J. Heikkinen: *ISIJ Int.*, **52** (2012), 2158.
2) C. E. Loo: YANDI Ore Utilization Handbook, BHP Billiton, Singapore, (2010), 41.
3) C. E. Loo, R. P. Williams and L. T. Matthews: *Trans. Inst. Min. Metall. C*, **101** (1992), C7.
4) R. M. German: Liquid Phase Sintering, Plenum Press, New York, (1985), 6.
5) C. E. Loo and W. Leung: *ISIJ Int.*, **43** (2003), 1393.
6) E. Kasai, Y. Omori and S. Wu: 5th Int. Symp. Agglomeration, IChemE, Rugby, (1989), 71.
7) G. Yap, B. Loo, N. Tame, H. See and T. Langrish: Chemeca 2007, Eng. Aust., Barton, (2007), 347.
8) P. R. Dawson, J. Ostwald and K. Hayes: *Proc. Australas. Inst. Min. Metall.*, **289** (1984), 163.
9) R. M. German: Sintering Theory and Practice, John Wiley & Sons, New York, (1996), 241.
10) K. Nakashima and K. Mori: *ISIJ Int.*, **32** (1992), 11.
11) K. C. Mills, L. Yuan and R. T. Jones: *J. South. Afr. Inst. Min. Metall.*, **111** (2011), 649.
12) K. C. Mills and B. J. Keene: *Int. Mater. Rev.*, **32** (1987), 1.
13) Slag Atlas, 2nd ed., ed. by VDEh, Verlag Stahleisen GmbH, Düsseldorf, (1995), 405.
14) T. Young: *Philos. Trans. R. Soc. Lond.*, **95** (1805), 65.
15) D. Bonn, J. Eggers, J. Indekeu, J. Meunier and E. Rolley: *Rev. Mod. Phys.*, **81** (2009), 739.
16) C. E. Loo and L. T. Matthews: *Trans. Inst. Min. Metall. C*, **101** (1992), C105.
17) R. M. German, P. Suri and S. J. Park: *J. Mater. Sci.*, **44** (2009), 1.
18) A. W. Adamson and A. P. Gast: Physical Chemistry of Surfaces, John Wiley & Sons, New York, (1997), 19.
19) S. Machida, K. Nushiro, K. Ichikawa, H. Noda and H. Sakai: *ISIJ Int.*, **45** (2005), 513.
20) C. W. Bale, E. Bélisle, P. Chartrand, S. A. Decterov, G. Eriksson, K. Hack, I.-H. Jung, Y.-B. Kang, J. Melançon, A. D. Pelton, C. Robelin and S. Petersen: *Calphad*, **33** (2009), 295.
21) L. Zhang, S. Jahanshahi, S. Sun, C. Chen, B. Bourke, S. Wright and M. Somerville: *JOM*, **54** (2002), 51.
22) S. Wright, L. Zhang, S. Sun and S. Jahanshahi: *J. Non-Cryst. Solids*, **282** (2001), 15.
23) C. E. Loo: *ISIJ Int.*, **45** (2005), 436.
24) D. Debrincat, C. E. Loo and M. F. Hutchens: *ISIJ Int.*, **44** (2004), 1308.
25) S. Sumita, K.-j. Morinaga and T. Yanagase: *J. Jpn. Inst. Met.*, **47** (1983), 127.
26) P. Vadász, M. Havlík and V. Daněk: *Can. Metall. Q.*, **39** (2000), 143.